

A NEW SETUP FOR THE STUDY OF ADSORPTION/DESORPTION PROCESSES AND NANOPARTICLES FORMATION IN POROUS ALUMINA

C. Marinelli,¹ E. Mariotti,¹ N. Papi,¹ F. Sarri,¹ A. Ziccardi,¹ R. Cecchi,¹ L. Stiacchini,¹ C. Viti,¹
A. Khanbekyan,² I. Gladskikh,³ P. Petrov,³ T. Vartanyan³

¹Department of Physical Sciences, Earth and Environment, Siena University, Italy; ²Department of Physics and Earth Science, Ferrara University, ³ITMO University, St. Petersburg, Russia

Abstract. We present a setup devoted to the study of adsorption and desorption processes of alkali atoms after deposition on a 300 nm thick porous alumina substrate in an Ultra High Vacuum chamber. Rubidium atoms, delivered by a dispenser source, enter the 20-30 nm diameter pores, diffuse in and stick to their walls. A 1 W power laser is used in order to induce detachment and take the atoms back in the vapor phase in a very tight confinement region. The desorbed atoms coming out the sample can be monitored via both a resonant optical detection and an electronic amplifier after ionization. The desorbing laser is also able to promote the formation of Rubidium nanoparticles, as the high Rb vapor density in the pores favors aggregation around nucleation point defects. In this way, the apparatus allows for the study of the fundamental processes related to atom – surface interactions in presence of light as well as of several promising application to nanomaterials.

Key words: Nanoparticles; Nanoporous materials; Adsorption and desorption; Atom - surface interaction; Laser spectroscopy; Adatoms

INTRODUCTION

Understanding the adsorption and desorption phenomena of atoms is a key factor to create, produce and grow new nanomaterials,¹⁻⁶ in a field where, in the last decade, a great impact on scientific research was given by a new generation of sensors, devices, drug-carriers etc. In particular, the study of atom adsorption and desorption mechanisms driven by light from a porous substrate can be a useful tool to manipulate the growth of nanoscaled clusters.⁷⁻⁹

The LIAD technique (Light Induced Atoms Desorption), discovered by Gozzini in 1994,¹⁰ is a powerful way to strongly modify the density of the desorbing species in a closed cell and can be used to create aggregates of alkali atoms in nanopore patterns, as demonstrated.¹¹ LIAD is a non-thermal and non-resonant effect, consisting in a sort of evaporation, promoted by light, of atoms and molecules that have been previously captured on a solid substrate surface. It was observed for the first time in a sodium vapor gas and later extended to all the alkali atoms such as rubidium, lithium, potassium, cesium and francium;¹²⁻¹⁵ it is anyway a universal effect, applicable to any atomic or molecular species, being unfortunately non-selective.

The desorption due to LIAD light can be explained with the interaction of the laser light interacts with atoms adsorbed on the surface. In the case of weak

chemical bonds, typical of physisorption mechanisms, after for example a PDMS (poly-dimethylsiloxane) wall coating procedure in an absorption cell, the light generated by any source (even non-coherent one) can very easily break the bond releasing the alkali atoms in vapor phase. This effect also proceeds when the interaction with the surface is stronger for about one order of magnitude:^{16,17} in that case, it is sufficient to either increase the light intensity or to make the whole available surface wider, as in nanoporous material.

Moreover, it has been observed that LIAD effect can favor, in the very small pore volume of a nanopore structured transparent sample, the self-assembly of alkali atoms and control their evaporation properties depending on the wavelength of the light used for the illumination of the desorbed species,¹⁸ showing a paramount importance for creation of alkali nanostructures.

The target of our work is 1) to study the dynamics of adsorption of rubidium in our samples; 2) to investigate the desorbing effect on rubidium atoms previously implanted in samples of porous alumina of different thicknesses (50 nm, 100 nm and 300 nm) when excited by a powerful either violet or green light source through LIAD effect; 3) to look for the eventual formation of Rb nanoclusters. The experiments are made in an open vacuum chamber, where we can monitor the most important parameters to optimize the process.

Correspondence to:

E. Mariotti

Department of Physical Sciences, Earth and Environment, Siena University, via Roma 56, 53100 Siena, Italy.

Tel.: +39.0577.234684

E-mail: mariotti@unisi.it

SAMPLE CHARACTERIZATION

The samples of porous alumina, whose stoichiometric formula is Al_2O_3 , consist in a layer of several tens of nanometers in thickness, prepared via a vacuum thin film deposition technique, and later annealed on a 10 mm diameter, 2 mm thick disk sapphire substrate. The 300 nm thick sample is shown in Figure 1, where the bluish color and the smaller diameter of alumina put in evidence, by eyes, the existence of the deposited film. The material is perfectly transparent in the visible region of the electromagnetic spectrum at a visual check.

The annealing process consists in a heat treatment to increase hardness and ductility of a material removing defects due mismatching from crystalline frameworks of sapphire and the amorphous nanostructure of porous alumina.

The declared size of the pores of the three samples of alumina is around 20-30 nm and it's going to be investigated by Transmission Electron Microscopy (TEM) only after this study as it requires the destruction of the sample itself.

Similar porous glass samples with the same features in terms of nanopore size have been checked by TEM technique. Figure 2, one of the pictures taken at the microscope, shows a representative TEM image of the porous glass, characterized by a "spongy-like" nanotexture with pores around 20 nm in size. The pores are interconnected, giving rise to a network of randomly oriented channels. The overall nanotexture is perfectly isotropic. The emptied solid matrix corresponds to a total internal surface of several square meters, where a huge number of atoms can be lodged. We have demonstrated in the past that atoms entering the pores can diffuse deeply inside and can be accumulated in the thin film, occupying more and more surface sites. Anyway, some of our measurements seem to tell us that the density rapidly drops as a function of the penetration depth.

This filling process is favored in a sealed cell, where the presence of a reservoir can continuously maintain the vapor density at the level imposed by the selected temperature (for rubidium, this means something in the order of 10^{10} atoms/cm³ just at room temperature), even if atoms are disappearing in the nanostructure in a "neverending" mechanism. This is not reproducible in an open chamber, as the connection to vacuum systems is a loss factor of atoms, as well as the very small ratio of the sample surface on the metal wall surface. Moreover, the stainless-steel sticking coefficient in an atom – wall collision is pretty close to one, and the atoms hitting the chamber are immediately lost from the vapor phase. In other words, in this kind of setup both the sample loading process and the detection of optical absorption or transmission signal is much more difficult. However, the apparatus

has other advantages: a) the flexibility, allowing different types of experiment, b) the complementarity of different possible detection techniques, c) the opportunity to study the sample outside the chamber, if properly treated, at the end of the experiment.

In Figure 3 the optical density spectrum for the 50 nm thick sample of alumina and for its substrate before and after the annealing procedure is shown. We remember that the Optical Density (OD), a dimensionless parameter, is defined as the natural logarithm of the ratio of incident to transmitted spectral intensity through a material. The sample is really transparent in the whole visible and infrared range of the electromagnetic spectrum. The presence of alumina creates a maximum in the transmission in the violet region, while the annealing method doesn't influence too much the optical response.



Figure 1. Picture of the 300 nm thickness nanoporous alumina sample. It is clearly visible a blueish layer corresponding to the deposited alumina.

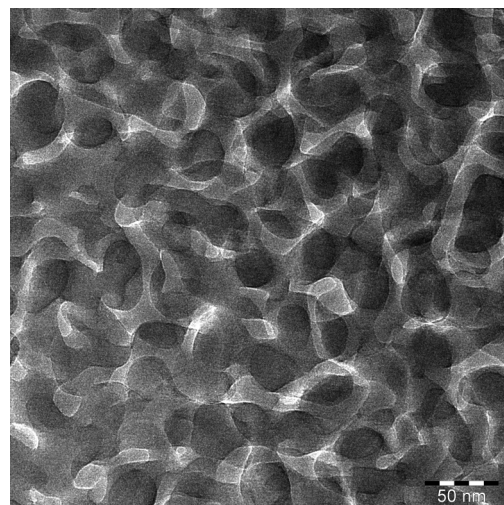


Figure 2. TEM image of nanopores in amorphous vitreous glass, the pores have a distribution in size with a medium value around 20 nm as declared by the manufacturer.

In Figure 4, the optical density responses of the alumina samples with 100 nm and 300 nm thicknesses are reported, as compared to their sapphire substrate. The graph shows that the transmission oscillates as it may be expected because of the interference effects in the thin porous layer that acts as antireflection coating for the optically denser bulk sapphire. We have not checked for the isotropy of our films but other authors claim that porous alumina show a preferential direction of the pore distribution.¹⁹

Experimental apparatus

The experimental setup is shown as a whole in Figure 5 and sketched in Figure 6.

It is mainly formed by a vacuum chamber, a low degassing stainless steel 6 way cross, completed by connection ports for the pressure measurement systems, the insertion of a feeded alkali dispenser, the sample manipulation, the optical windows for absorption/reflection/transmission of light beams, the analysis instrumentation.

The pressure inside the chamber is below 10^{-7} mbar, as provided by both a small turbomolecular vacuum pump, that needs a continuous outflow by a mechanical rotary pump, and an ionic pump.

The samples described in the previous paragraph can be placed at the center of the chamber by a translating and rotating aluminum holder, connected to a through vacuum flange, prepared in our mechanical workshop. The rubidium dispenser is an Italian trademark able to release a variable quantity of atoms in the vapor phase when it is heated by Joule effect via an electric current in the range 0-6 A. One can modulate the atom flux by changing the temperature (current) value. In fact, the dispenser is connected via a feedthrough flange to a continuous current stabilized power supply, and is placed in such a way that the minimum distance to the sample can be a few centimeters, as shown in Figure 7. The rotating support allows us to vary the angle for

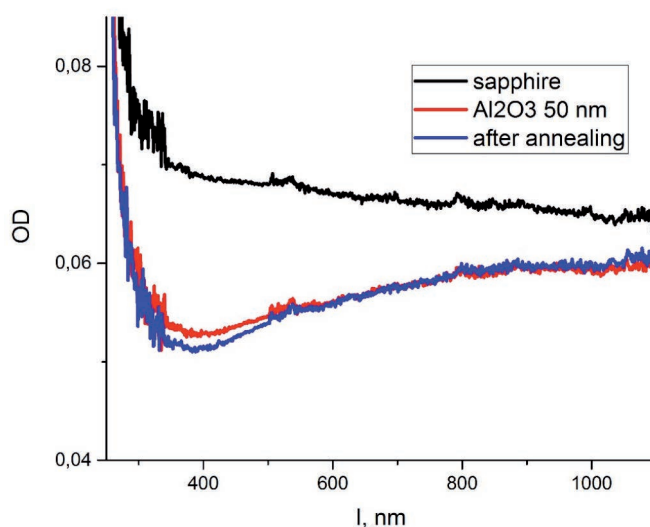


Figure 3. Spectrum of optical density for the sapphire substrate (black curve), after deposition on it of a 50 nm thick alumina sample (red curve) and after the annealing procedure (blue curve).

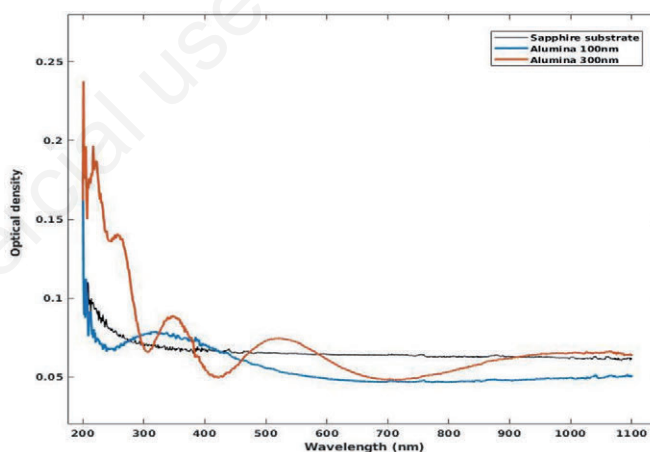


Figure 4. Optical density spectrum for alumina samples with 100 nm (blue curve) and 300 nm (orange curve) thickness and for the sapphire substrate (black curve).

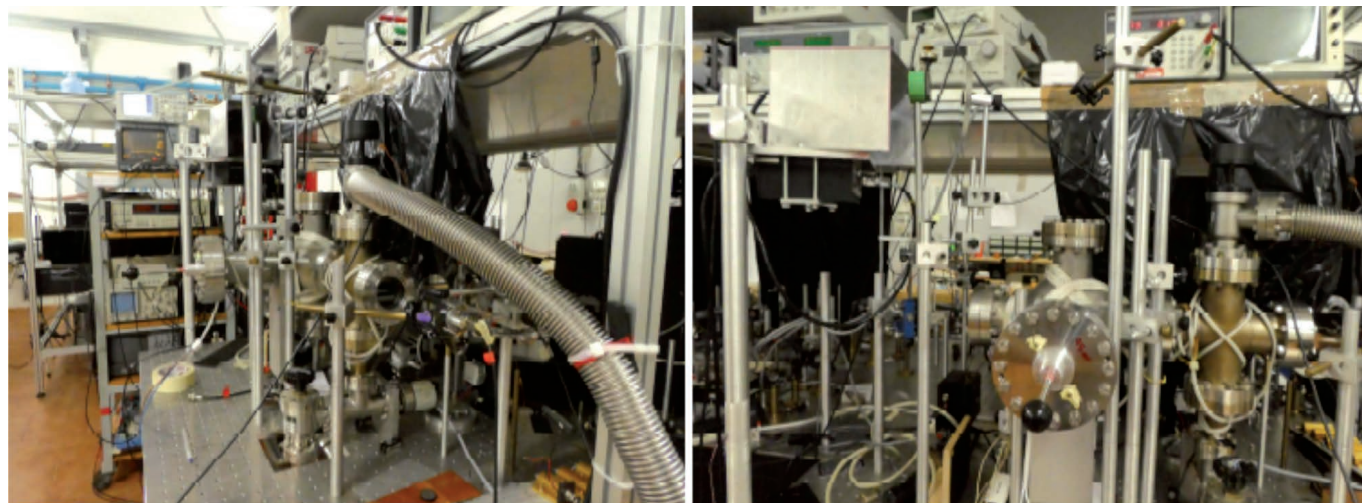


Figure 5. Pictures of the setup.

the exposure to Rb dispenser as well as the angle towards the LIAD laser beam and the electronic detection system.

A near infra-red diode laser is tuned to the Rb D₂ line at 780 nm. Its wavelength is scanned across the resonance by a triangular waveform generator voltage in order to change the current in the semiconductor chip forming the laser. This parameter modifies by a fine tuning the output laser frequency, and the useful scan can be wider than 10 GHz, to be compared with the 384 THz frequency of the atomic transition.

The propagating probe beam is split before entering the vacuum chamber through a high-quality optical window on a flange; a first beamsplitter sends a small portion of the intensity to a sealed reference cell, behind which the transmitted signal is detected by a photodiode in order to look for and continuously check the presence and the position of the Rb resonance.

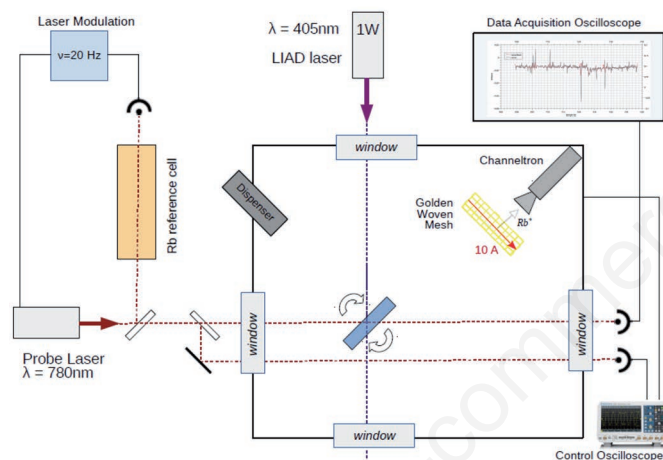


Figure 6. Simplified scheme of the experimental apparatus. In dashed red the probe laser beams. In dashed violet the desorbing laser beam.

If the frequency is correct, in presence of rubidium, the absorption signal shows the D2 Doppler broadened peaks of the natural mixture of isotopes of 85 and 87 a.m.u., as shown in Figure 8, together with the energy level scheme for the ground and first excited states.

A second beam splitter divides again the main beam in an upper beam hitting the sample and propagating close to the dispenser and a lower beam passing below the sample.

The first probe is a way to check A) the dispenser delivery of atoms to the sample; B) the scattering of atoms by the sample during the loading process; C) the change in reflectivity and transmittivity of the sample; D) the presence of desorbed rubidium atoms after an illumination with a desorbing light beam.

The second probe mainly controls, in the previous case D), the eventual unwanted absorption signal due to rubidium atoms coming from the rest of the chamber

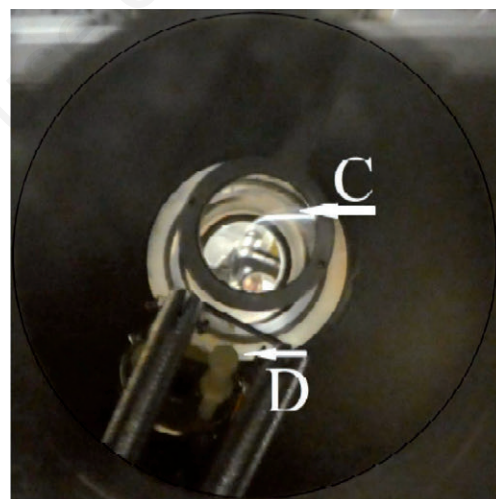


Figure 7. Picture of the sample in the chamber; the strip below the sample is the Rb dispenser.

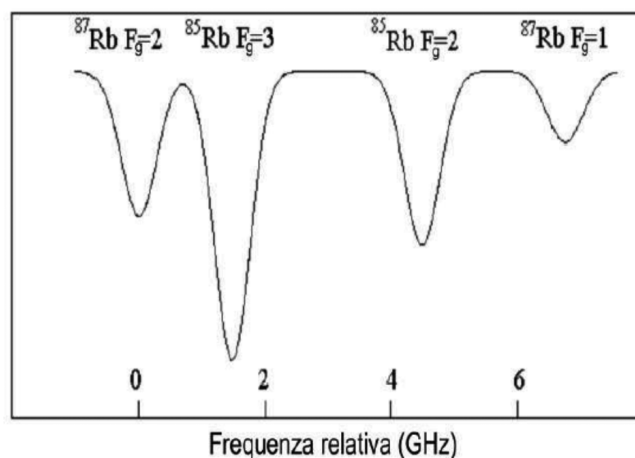
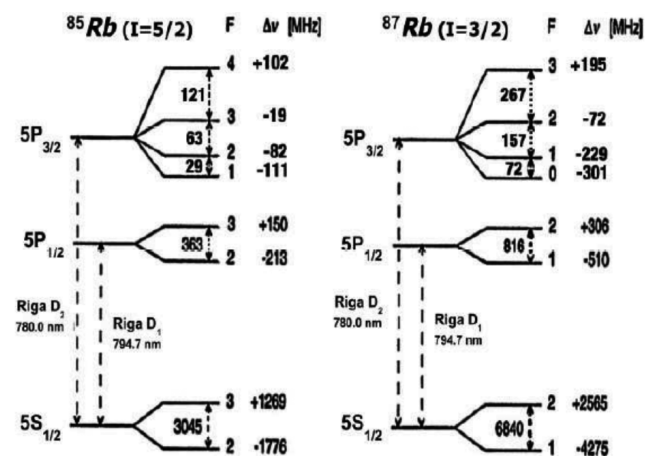


Figure 8. The scheme of the D₂ and D₁ lines of ⁸⁷Rb and ⁸⁵Rb (left); Experimental recorded spectrum for D₂ line of natural mixture of Rb isotopes (right).

surface, as desorbed by some scattered light. Such a contribution should make us suspicious about the simultaneous signature of absorption on the first probe beam.

The acquisition can be performed either by a direct transfer of an oscilloscope saved spectrum or by a LabView dedicated software allowing for the selection of the signal on one of the absorption peaks in order to get its time evolution and to study the corresponding dynamics, with a time resolution of about 2 ms.

By this second choice, the final graph gives the atomic density, that is only in a first approximation proportional to the absorption signal. In fact, the program automatically inverts the exponential Beer's law, taking a reference value for the absorption in a spectral region external to the atomic resonance.

Due to the low signal to noise ratio value (S/N), as a consequence of the few atoms usually involved in the studied processes, it is necessary to introduce a post-analysis statistical smoothing procedure on the data.

In Figure 9 we report on a comparison between the absorption signals from the reference cell and from the vacuum chamber, as taken when the dispenser is on.

It should be noted that, even if the total path inside the chamber is much longer than in the reference cell, the absorption signal is much lower: the dispenser is

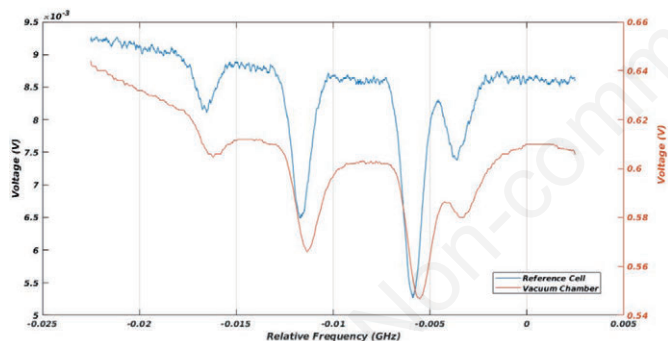


Figure 9. Recorded spectrum of Rb in: the reference cell (upper curve) and the vacuum chamber at dispenser on (lower curve).

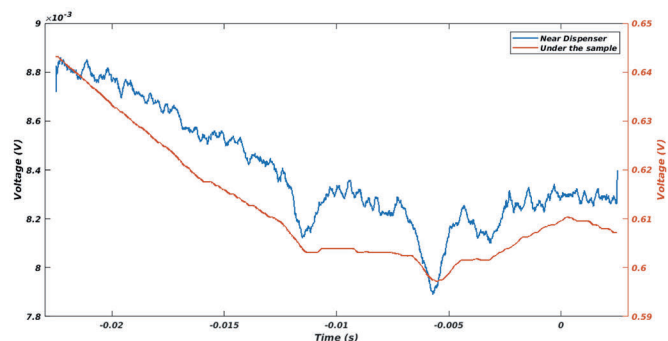


Figure 10. Recorded spectrum of Rb for the two laser beams in the vacuum chamber at dispenser.

not able to reproduce the density condition typical for a saturated vapor at room temperature. It is interesting to point out that the peak maxima are not in the same frequency position: this is a signature of the effect of optical pumping, a mechanism of accumulation of population in energy levels non-interacting with the light beam that is conserved only for coated surfaces, as in the case of the reference cell, where PDMS is present. This behavior has been recently studied by us in detail.²⁰

In Figure 10 a comparison of the signals for the beams crossing the chamber in different positions (blue, over the sample, red, below the sample) is shown, again, with the dispenser on. In this case it has to be stressed that, even after a long rubidium delivery time, the density is non-homogeneous in the chamber: the dispenser creates a wide-angle atomic beam instead of being an effusive oven.

By the LabView program it is possible to get registrations of the dynamics of the dispenser switching on and off, as shown in Figure 11. In the first case, it is possible to see as the dispenser, suddenly crossed by the maximal current, produces a vapor cloud as due to an apparent non-homogeneous increase of temperature and of atom release. On the contrary, the cooling is rapid and the atomic density goes back to zero in a few seconds, with a much cleaner S/N.

In order to check the deposition of rubidium in the porous alumina, an intense laser light beam is sent on the sample via the upper window of the chamber. We can use either a duplicated solid state laser in the green, at 532 nm, or a violet diode laser at 405 nm. These light sources induce desorption of atoms embedded in the sample after a deposition procedure, as mentioned in the introduction.

Again, one can optically monitor the desorbed Rb atoms as a reduction of transmittance of the probe laser. The laser beams have been expanded via a lens in order to maximize the illuminated sample surface, without having scattered light by the holder and by the chamber walls.

At the moment, we have tried a few loading procedures. Only for a time prolonged over the 2 hours and at the maximum dispenser current, we got an optical detection of atoms desorbed by the green light at 1 W of power. The measurement has been performed after the recovering of the initial vacuum condition: in fact, the presence of rubidium vapor by the dispenser modifies the internal pressure for a factor around 5. The signal is shown in Figure 12 and refers to a loading time of 3h30 .

Even though the signal is noisy also after the smoothing (obtained by a moving average algorithm), it is still visible a steep reduction (in a millisecond range) for a factor 3 in the transmittance of the probe beam at the time when LIAD diode laser hits the sample. This emission of atoms lasts for about 15 milliseconds, after which the rubidium atoms are

captured by the vacuum pumping system and adsorbed by the wall of the chambers and density goes back to zero. It is evident from this result that the number of atoms on the surface and in the first pore volume is pretty low, that the laser completely depletes the samples: in these conditions, and that the optical detection method is at the limit of sensitivity.

The repeated use of the dispenser has produced its exhausting. We had to replace it by opening the chamber: in this way the samples have been oxidized and had to be replaced, too.

For a more efficient and complementary detection, we have mounted in the chamber an electronic system. It is mainly composed by a channel electron multiplier (C.E.M.), or channeltron, *i.e.* a device able to amplify any ion signal up to a factor 10^8 . This component detects charged particles: we have to ionize rubidium atoms in order to get the signal. This is accomplished

by a Golden Woven Mesh, where the atoms are captured after the desorption or in the scattering by the sample; another high voltage power supply can heat the mesh, that emits by thermoionic effect the ionized particles. For this system a new handmade support connected to a dedicated feedthrough flange was built, as shown in Figure 13.

The phenomenon is governed by Saha-Langmuir equation, giving the ratio of ionized (n_+) versus neutral (n_0) density in terms of the following parameters:

$$\frac{n_+}{n_0} \propto e^{(\phi-I)/kT}$$

ϕ the work function of gold, I , the first ionization potential of Rb, k , the Boltzmann's constant and T , the temperature of the mesh. For the gold mesh used the work function is equal at 5.30-5.40 eV, depending on its temperature, and for Rb atom the first ionization potential I value is 4.18 eV.

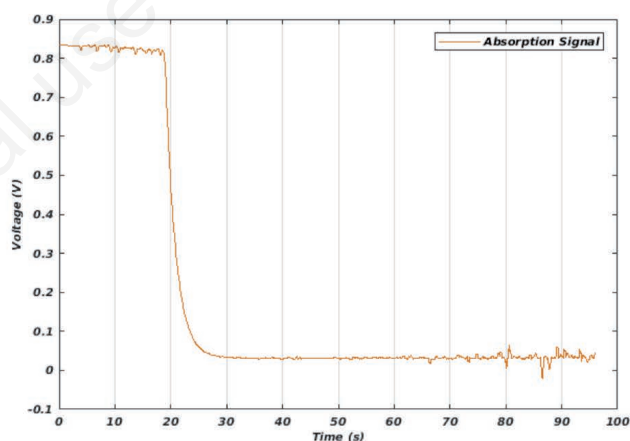
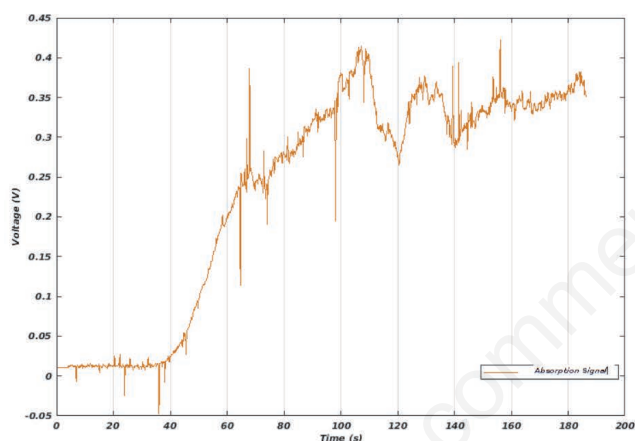


Figure 11. Dynamics of the peak absorption signal in the vacuum chamber when the the dispenser is switched on (left) and off (right).

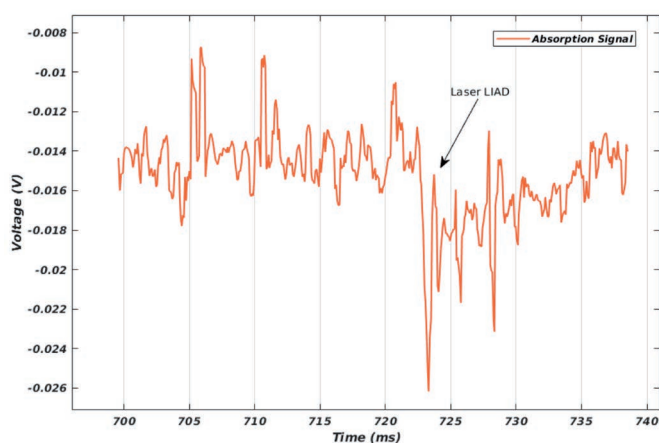


Figure 12. Dynamics of the desorbed Rb atoms from the sample as induced by a 1 W, 532 nm laser (switched on around $t=720$ ms).



Figure 13. Homemade channeltron and Golden Woven Mesh holder lodged in a feedthrough flange (maximum current 10 A) for the vacuum chamber.

The collected ions are amplified and an electronic signal can be sent to an oscilloscope or to a converter. We are still checking the response of this detector: till now, it has been seen the signal coming from the "dirty" mesh. This test period will be also useful to clean the mesh: as mentioned, we have not real selectivity on the gold emission, and the best solution is a cross check with the optical one.

CONCLUSIONS

We have arranged a new apparatus for the study of adsorption and desorption processes and their dynamics for rubidium, or, more generally, for alkali atoms loaded on a porous nanostructured sample. The system allows for different types of detection: the species selective optical detection by absorption and/or transmission signals, the very sensitive electronic detection via ionization and channeltron measurement. At the moment the setup has been completed and preliminary measurements of the rubidium loading process of the sample, of the ionized rubidium signal from the charge amplifier and of the desorption of rubidium by a powerful violet laser beam have been obtained.

ACKNOWLEDGMENTS

The St. Petersburg group is grateful for the financial support to RFBR (17-52-18037) and the Ministry of Education and Science of Russian Federation (3.4903.2017/6.7).

REFERENCES

1. Zeng X, Chen C, Zheng S, et al. Corrigendum: Rapid in situ synthesis of silver nanoparticles on the distal facet of a fiber by laser-induced photo-reduction. *Laser Phys Lett* 2014;11:016003.
2. MacDonald KF, Fedotov VA, Pochon S, et al. Optical control of gallium nanoparticle growth. *Appl Phys Lett* 2002;80:1643-5.
3. Callegari A, Tonti D, Chergui M. Photochemically Grown Silver Nanoparticles with Wavelength-Controlled Size and Shape. *Nano Lett* 2003;3:1565-8.
4. Fedotov VA, MacDonald KF, Zheludev NI. Light-controlled growth of gallium nanoparticles. *J Appl Phys* 2003;93:3540-4.
5. Soares BF, MacDonald KF, Fedotov VA, Zheludev NI. *Nano Lett* 2005;5:2104-7.
6. Srivastava S, Santos A, Critchley K, et al. Light-controlled self-assembly of semiconductor nanoparticles into twisted ribbons. *Science* 2010;327:1355-9.
7. Slepikov AD, Bhagwat AR, Venkataraman V, et al. Generation of large alkali vapor densities inside bare hollow-core photonic band-gap fibers. *Opt Express* 2008;16:18976.
8. Bhagwat AR, Slepikov AD, Venkataraman V, et al. On-demand all-optical generation of controlled Rb-vapor densities in photonic-band-gap fibers. *Phys Rev A* 2009;A79:063809.
9. Vartanyan TA, Khromov VV, Leonov NB, Przhibel'skii SG. *Proc SPIE* 2011;7996:79960H.
10. Gozzini A, Mango F, Xu J, et al. Light-induced ejection of alkali atoms in polysiloxane coated cells. *Nuovo Cimento D* 1993;15:709-722.
11. Burchianti A, Bogi A, Marinelli C, et al. Reversible Light-Controlled Formation and Evaporation of Rubidium Clusters in Nanoporous Silica. *Phys Rev Lett* 2006;97:157404.
12. Marinelli C, Burchianti A, Bogi A, et al. Desorption of Rb and Cs from PDMS induced by non resonant light scattering. *Eur Phys J* 2006;D37:319-25.
13. Barker DS, Norrgard EB, Scherschligt J, et al. Light-induced atomic desorption of lithium. Available from: <https://arxiv.org/pdf/1805.09862.pdf>
14. Gozzini S, Lucchesini A. Light-induced potassium desorption from polydimethylsiloxane film. *Eur Phys J* 2004;D28:157-62.
15. Agustsson S, Bianchi G, Calabrese R, et al. Enhanced Atomic Desorption of 209 and 210 Francium from Organic Coating. *Sci Rep* 2017;7:4207.
16. Bonch-Bruevich AM, Vartanyan TA, Gorlanov AV, et al. Photodesorption of sodium from the surface of sapphire. *Sov Phys JETP* 1990;70:604.
17. Bonch-Bruevich AM, Vartanyan TA, Maksimov YN, et al. Photodesorption and work function study of long-living excited electronic states on metal surfaces. *Surf Sci* 1994;307-309A:350-4.
18. Marmugi L, Mariotti E, Burchianti A, et al. Laser-driven self-assembly of shape-controlled potassium nanoparticles in porous glass. *Laser Phys. Lett* 2014;11:085902.
19. Villalba S, Failache H, Lezama A. Light-induced atomic desorption and diffusion of Rb from porous alumina. *Phys Rev A* 2010;81:032901.
20. Krasteva A et al. Dynamics of optical pumping processes in coated cells filled with Rb vapor, in preparation.